The age and depth of exhumed friction melts along the Alpine fault, New Zealand

L.N. Warr
Centre de Géochimie de la Surface (CNRS-ULP), 1 rue Blessig, 67084-Strasbourg, France
B.A. van der Pluijm
S. Tourscher
Department of Geological Sciences, University of Michigan, Ann Arbor, Michigan 48109, USA

ABSTRACT

Laser-ablation $^{40}Ar/^{39}Ar$ step-heating analyses of 20 pseudotachylyte veins from a single location along the exhumed central portion of the active Alpine fault of New Zealand yield total gas age values between 1 and 19 Ma. Evidence shows that they are genetically related and were formed during coeval episodes of seismogenic melting at shallow crustal depth, contrasting with a spread in formation ages. The total gas ages show an exponential decrease with increasing proportion of melt matrix and K content, reflecting incomplete degassing and mixtures of radiogenic Ar sources. Calculation of intercepts for all–melted matrix and all–clast end-member components indicate ca. 570 ka (Quaternary) friction-melting ages of ca. 332 Ma (Lower Carboniferous) source rock. Assuming an average exhumation rate of 6–9 mm/yr for uplift and erosion, these results imply that friction melts were generated during major slip episodes at ~3.5–5 km crustal depth. We conclude that reliable dating of young pseudotachylyte can be accomplished by combining chronologic study with clast-matrix quantification of genetically related vein assemblages.

Keywords: $^{40}Ar/^{39}Ar$ dating, pseudotachylyte, coseismic faults, friction melt, Alpine fault.

INTRODUCTION

Pseudotachylyte, the product of friction melting during large-magnitude earthquakes, provides a unique opportunity to study the mechanism, age, and location of coseismic faulting (Sibson, 1975; Di Toro et al., 2006). These clast-ridden melts are known to form under a variety of conditions, ranging from deep-crustal faulting to landslides at the surface (Masch et al., 1985; Magloughlin and Spray, 1992). Despite their diverse occurrence, it remains a key challenge to isotopically date these melts and catalog large paleoseismic events of the geological record in time and space. In cases where the rate of fault exhumation is constrained, accurate age determinations of pseudotachylyte can also provide depth estimates for friction melting.

The principal method used for dating friction melts in crustal fault zones is the $^{40}Ar/^{39}Ar$ isotopic technique, determined by step-heating or laser-ablation methods (Merrihue and Turner, 1966; Magloughlin et al., 2001; Sherlock and Hetzel, 2001; Mueller et al., 2002; Di Vincenzo et al., 2004). Determining true formation ages requires that (1) all inherited radiogenic Ar is outgassed from both melt and clast components, (2) no radiogenic Ar is lost after quenching, and (3) no externally derived excess Ar gas accumulates in the sample following crystallization. In the case of natural pseudotachylytes, these conditions are commonly not fulfilled due to the incomplete and heterogeneous nature of flash melting and the trapping of Ar-bearing fluid inclusions in clasts (Di Vincenzo et al., 2004).

The complexities of interpreting "apparent age spectra" of friction melting is mirrored both by the relative rarity of simple degassing curves that show well-defined plateau ages and by the significant variations in total gas age measured on pseudotachylyte veins (Kohut and Sherlock, 2003). Despite these problems, significant age determinations have been obtained by laser-probe dating of melted matrix and assessment of mixed Ar sources as indicated by elevated Ca/K and Cl/K ratios (Sherlock and Hetzel, 2001; Mueller et al., 2002). The successful dating of young pseudotachylytes presents a particular challenge because the amount of radiogenic Ar is too low for effective laser probing of the vein matrix. Here, $^{40}Ar/^{39}Ar$ laser-ablation study of small matrix-rich rock fragments appears to be the best approach (Magloughlin et al., 2001; Warr et al., 2003).

In this study, we examine $^{40}Ar/^{39}Ar$ variations of 20 geologically young pseudotachylyte veins collected from a single location along the central section of the Alpine fault, New Zealand, in order to determine the true age and crustal depth distribution of friction melting. This area is of interest because previously analyzed pseudotachylytes have displayed a large range of isotopic ages in well-developed veins (Adams, 1981; Warr et al., 2003), and the region has a well-constrained exhumation history over the last 5 m.y. (Batt et al., 2000). Our objective was to test whether the friction melts of seemingly different ages were generated at various crustal depths or whether the melts were coeval and formed at a specific time and depth during the exhumation history of the fault. The latter would require an alternative explanation for the range in observed ages that is not related to variable-depth melting. Based on the mineralogic, isotopic, and geochemical variations found during this study, we demonstrate that all sampled pseudotachylytes are genetically related and formed during the Quaternary, within a single shallow-crustal generation zone along the Alpine fault.

GEOLOGICAL SETTING AND PSEUDOTACHYLYTE SAMPLES

The Alpine fault represents an active, oblique-slip segment of the Australia-Pacific plate boundary (Fig. 1A). The central section is characterized by a steep thrust geometry with high rates of dextral strike-slip displacement (27 ± 5 mm/yr) and rapid exhumation of Pacific hanging-wall rocks at rates as high as 10 mm/yr (Cooper and Norris, 1994; Norris and Cooper, 2001).

The 20 pseudotachylytes analyzed here were collected to the east of Hari Hari, mainly from boulder material washed down from the fault trace along Harold Creek (Fig. 1A). Fault zones exposed in large boulders typically contain parallel sets of thin planar melt-generation

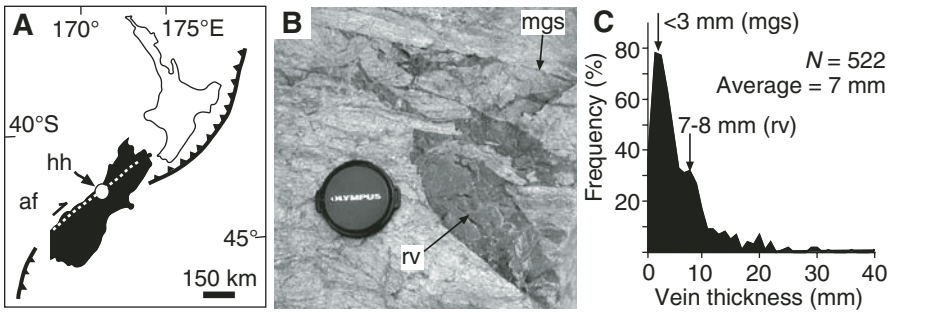

Figure 1. A: Map of New Zealand showing location of pseudotachylytes (white point) collected at Harold Creek, along the Alpine fault (af); hh—town of Hari Hari. B: Irregular-shaped, thick reservoir veins (rv) formed adjacent to a set of melt-generation surfaces (mgs). C: Vein thickness frequency plot based on measurements of pseudotachylyte exposed in stream boulders.

surfaces (<3 mm thick) that lie concordant to the lithological layering and thicker (average of 7 mm) offshooting reservoir veins (Figs. 1B and 1C). The melts were derived from mylonitized amphibolite quartzofeldspathic schists of the garnet-oligoclase zone, which represent metamorphosed graywacke lithologies of the Alpine schist (Grapes, 1995). The high silica content of the host rock represents intermediate to felsic compositions (Warr and van der Pluijm, 2005).

The fault rocks of the Hari Hari section lie at the northeastern end of the highly exhumed central section of the Alpine fault. Based on low $^{40}Ar/^{39}Ar$ hornblende ages as young as 3–5 Ma at the Franz-Josef Glacier, Little et al. (2005) estimated a maximum time-integrated exhumation rate of ~6–9 mm/yr for this section. This is in accordance with the high late Quaternary dip-slip rate of >12 mm/yr at Gaunt Creek and the 7–9 mm/yr regional uplift rate determined from displaced postglacial marine/terrestrial sediments of the Paringa River (Cooper and Norris, 1994; Norris and Cooper, 2001).

ANALYTICAL METHODS

Rock slabs oriented perpendicular to vein margins were cut from sample blocks. Polished thin sections were prepared for optical and scanning-electron microscopy (SEM), and backscattered-electron (BSE) images were obtained by traversing across the veins at a magnification of 500×. The relative abundance (%) of clast and matrix components was measured following the procedure outlined in Warr and van der Pluijm (2005) using area-related parameters of the National Institutes of Heath (NIH) Image Analysis software (http://rsb.info.nih.gov/nih-image/). The method effectively separates the larger quartz and feldspar clasts from very fine-grained, phyllosilicate-rich, neocrystallized matrix.

Powder preparations of the vein material were analyzed by X-ray diffraction to determine the principal mineral assemblages and by inductively coupled plasma–optical emission spectroscopy (ICP-OES) to quantify elemental concentrations. For geochemical analyses, samples were fusion digested using $LiBO_2$, and the analytical results were corrected for volatile content determined from loss-on-ignition. The K concentration used in this study, expressed as wt% K_2O, was calibrated against U.S. Geological Survey standards (rgm-1a, qlo-1, SDC-1 and bhvo-1).

Laser-ablation $^{40}Ar/^{39}Ar$ step-heating analysis of millimeter-sized (~0.01 g) rock chips selected to minimize clast content followed the procedure used by Lo Bello et al. (1987) and Magloughlin et al. (2001). An initial test of encapsulated verses noncapsulated samples showed consistency between total gas ages and Ar-retention ages, indicating that recoil effects were negligible. The fraction of cumulative $^{39}Ar_{(K)}$, $^{38}Ar_{(Cl)}$, and $^{37}Ar_{(Ca)}$ released during step heating was used to establish ^{39}Ar, Ca/K, and Cl/K degassing spectra, following application of correction factors. A summary of the results is given in Table 1, and further details are provided in the GSA Data Repository.[1]

RESULTS

The pseudotachylyte veins consist of a matrix composed of quartz-plagioclase-biotite with opaques and occasional chlorite. Common opaque phases are magnetite and ilmenite. Minor amounts of hornblende were detected only in sample pst6–2. Clast components consist of quartz, plagioclase, and some opaque minerals; the matrix-poor sample of pst4–1 is the only sample where phyllosilicate phases were observed in clast form. Based on unpublished microprobe data, the principal K-bearing mineral phase of these samples is neocrystallized biotite (mean of 9 wt% K_2O) and clasts of plagioclase feldspar (mean 0.12 wt% K_2O). Feldspar contribution to the ^{39}Ar signature is most significant in the K-poor veins (pst4–1 and pst24–1), with high (>5) Ca/K ratios for these samples.

The proportion of matrix and clast components determined for 12 of the 20 veins, expressed as percent matrix, ranges between 48% and 89% (Table 1). The matrix-rich samples are veins containing the most biotite, as indicated by the good correspondence between percent matrix and K_2O content. The K_2O ranges from 0.32 wt% K_2O in the sample characterized by 47% matrix (pst4–1) to 4.37 wt% K_2O for the 89% matrix-rich vein (pst9–1).

The $^{40}Ar/^{39}Ar$ total gas ages range from old values of 18.63 ± 0.23 Ma for the matrix-poor, low-K_2O sample (pst4–1) to young ages of 0.95 ± 0.23 Ma for the matrix and K_2O-rich vein of pst9–1. The ^{39}Ar spectra show a range of degassing patterns that can be grouped into three types: saddle, stepped, and pseudo-plateau shapes (Figs. 2A–2C). Saddle-shaped spectra are the most common (11 of the 20 samples) and characterize the full range of total gas ages measured. The oldest age spectra show very pronounced troughs whereby very old age values correspond to the early and late stages of ^{39}Ar release (approaching 180 Ma in Fig. 2A).

TABLE 1. ANALYTICAL RESULTS

Sample	% matrix	K_2O (wt%)	TGA (Ma)	Mean Ca/K	Cl/K
pst2–1	88	3.18	1.08 ± 0.01	0.40	0.004
pst2–2	78	2.55	1.73 ± 0.02	0.40	0.005
pst2–3	78	2.55	2.23 ± 0.05	1.00	0.005
pst3–1	74	1.34	4.71 ± 0.05	2.04	0.007
pst3–2	48	0.82	12.61 ± 0.14	3.30	0.008
pst3–3	58	0.83	8.73 ± 0.15	2.88	0.009
pst4–1	47	0.32	18.63 ± 0.23	7.28	0.025
pst9–1	89	4.37	1.12 ± 0.01	0.16	0.004
pst10–2	80	2.21	2.36 ± 0.03	0.84	0.004
pst10–3	80	2.29	2.95 ± 0.04	0.82	0.005
pst13–1	69	1.82	4.25 ± 0.05	1.85	0.006
pst14–1	88	3.40	0.95 ± 0.02	0.37	0.004

Note: Table shows summary of results for the 12 pseudotachylyte veins studied in detail. The % of matrix was measured by image analysis of scanning-electron microscope (SEM) backscattered images. The weight % (wt%) of K_2O was determined by inductively coupled plasma–optical emission spectroscopy (ICP-OES). The total gas age (TGA) and the mean Ca/K and Cl/K ratios were calculated from the concentrations of ^{40}Ar, ^{39}Ar, ^{38}Ar, and ^{37}Ar isotopes (full version of table is available in the GSA Data Repository; see text footnote 1).

[1]GSA Data Repository item 2007051, summary of mineralogical, geochemical, and isotopic results for the 20 pseudotachylyte veins (a more detailed version of Table 1), is available online at www.geosociety.org/pubs/ft2007.htm, or on request from editing@geosociety.org or Documents Secretary, GSA, P.O. Box 9140, Boulder, CO 80301, USA.

These peak ages correspond to elevated Ca/K and Cl/K ratios and indicate significant quantities of inherited Ar, probably present in the clast fraction. Stepped profiles characterize five veins that yield younger total gas age values (2.36–6.36 ± 0.05 Ma). The progressive increase in the fraction of degassed ^{39}Ar with increasing temperature (Fig. 2B) likely reflects mixtures of inherited Ar and perhaps internally sourced Ar that was not degassed during the friction-melting episode. Pseudo-plateau–type spectra characterize four veins that range in age from 0.95 to 4.71 ± 0.05 Ma. These patterns are defined by constant degassing of ^{39}Ar observed over ~35%–60% of the release spectra and usually correspond to plateaus in the Cl/K spectra (Fig. 2C).

Correlation plots between the total gas ages, percent matrix, and K_2O content reveal systematic, exponential relationships between these parameters (Figs. 3A–3C). The good correlation curve ($R^2 = 0.94$, $n = 12$) fitting $\exp(\lambda t) - 1$ (λ = decay constant, t = total gas age) against percent matrix yields well-defined y-axis intercepts equivalent to an age of ca. 570 ka for 100% matrix and ca. 332 Ma for 0% matrix (all-clast) end members (Fig. 3A). An exponential decrease in $\exp(\lambda t) - 1$ is also observed with increasing K_2O content ($R^2 = 0.90$; $n = 12$). Here, the fitted curve predicts veins with total gas ages of ca. 570 ka and 100% matrix would be characterized by >4.3 wt% K_2O content (Fig. 3B). An exponential increase in K_2O content also corresponds to the increasing percent of matrix (Fig. 3C; $R^2 = 0.90$; $n = 12$). Linear trends are observed when the total gas age is plotted against Ca/K and Cl/K ratios ($R^2 = 0.91$ and 0.66, respectively; $n = 20$), and the more reliable of the two regression lines intercepts zero at the same approximate age as the 100% matrix value of Figure 3A.

DISCUSSION AND CONCLUSIONS

The suite of pseudotachylyte veins studied from a single location along the rapidly exhumed, central section of the Alpine fault is characterized by large variation in total gas ages (ca. 1–19 Ma), percent matrix (48%–89%), and K content (0.32–4.37 wt% K_2O), showing well-defined exponential relationships. The occurrence of complex degassing spectra and age values well in excess of the regional background levels of biotite cooling ages (<2 Ma; Batt et al., 2000) indicates that many of the veins contain significant quantities of inherited Ar. Similar patterns have been described in the host rock mylonite schist of a pseudotachylyte from this location (Warr et al., 2003) with total gas ages of ca. 9.5 Ma and older, which were attributed to the occurrence of excess Ar. Ages approaching 180 Ma during the early and late stages of ^{39}Ar release (Fig. 2A) and the correspondence of

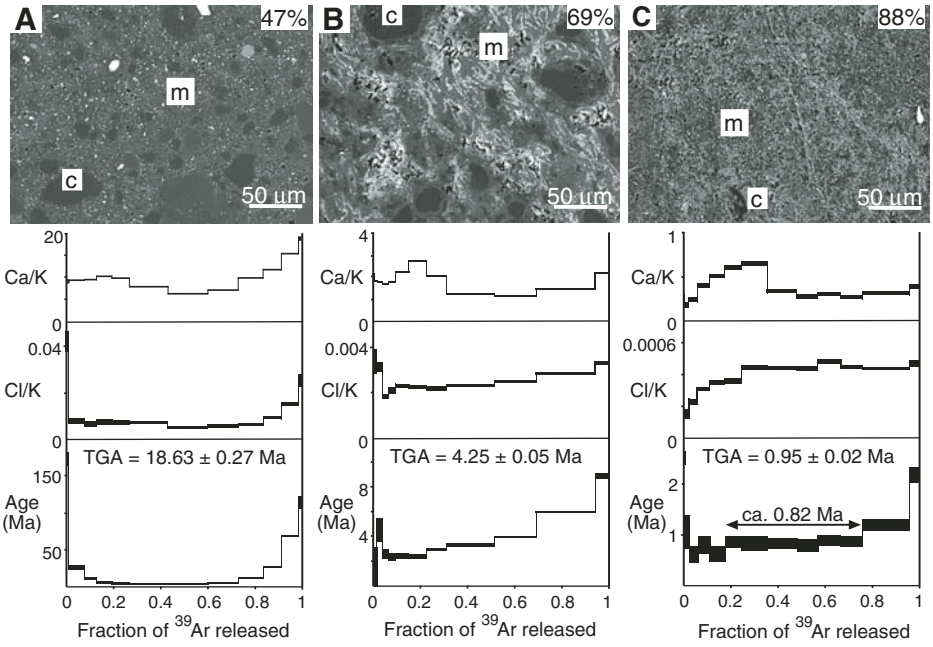

Figure 2. Backscattered-electron (BSE) images (magnification 500×) and "apparent-age spectra" of pseudotachylyte veins for (A) 47% (pst4–1), (B) 69% (pst13–1), and (C) 88% (pst2–1) matrix content. Clasts (c) are composed of either quartz (dark gray) or feldspar (medium gray); m—matrix; TGA—total gas age.

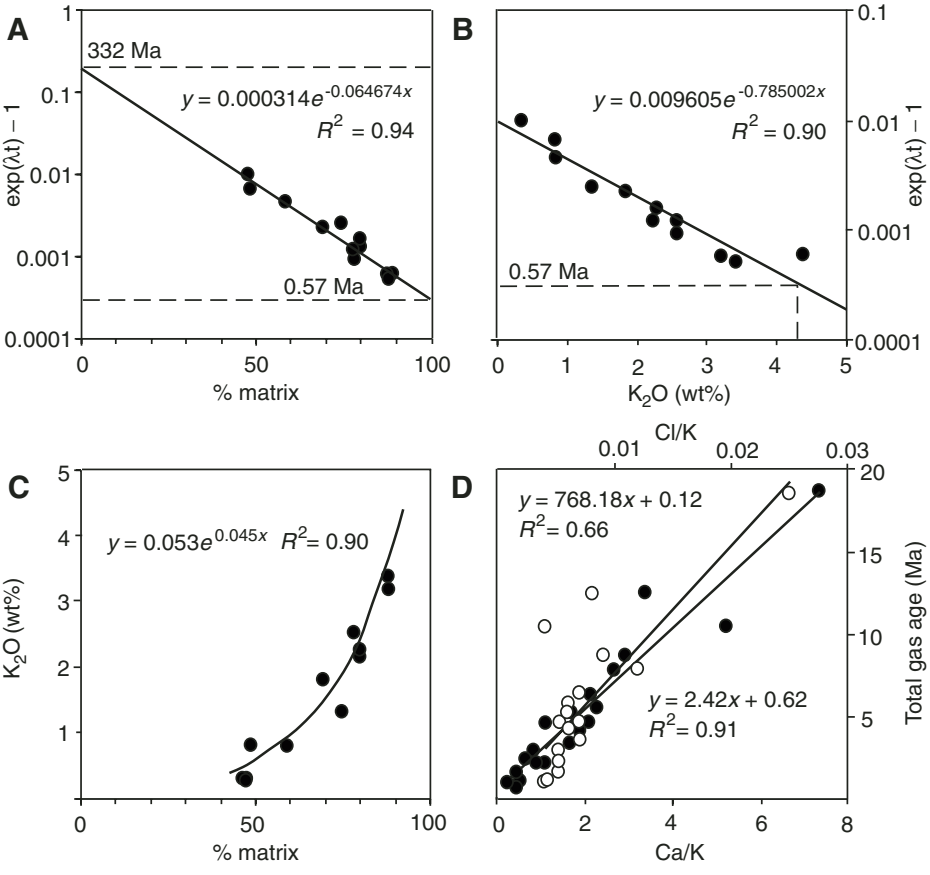

Figure 3. (A–D) Plots showing variation in total gas age, percent matrix, wt% K_2O, Cl/K, and Ca/K values. A and B plot ages expressed as $\exp(\lambda t) - 1$, where λ is decay constant of 0.0005543 and t is total gas age (TGA).

old ages to quartz-feldspar lithologies (i.e., low K_2O, high Ca/K and Cl/K ratios) imply an old Ar component, probably both within secondary fluid inclusions trapped in quartz (Di Vincenzo et al., 2004) and within thermally stable clasts. However, since the amount of inherited Ar decreases consistently with the increase in percent melt matrix, the bulk component of inherited Ar appears to have been introduced into the system prior to friction melting and not during subsequent alteration.

The curve of $\exp(\lambda t) - 1$ versus percent matrix (Fig. 3A) is best explained by the mixing of a two-component system that contains an old ca. 332 Ma inherited Ar age (intercept at 100% clast) and a young radiogenic age of ca. 570 ka (intercept at 100% matrix). The Lower Carboniferous date of ca. 332 Ma reflects the inherited Ar component, which represents a detrital age in accordance with provenance from the Carboniferous to Triassic New England orogen in northeastern Australia (Pickard et al., 2000). The fact that this component has not been reset during amphibolite metamorphism and the detrital signature is strongest in quartzofeldspathic lithologies with high Ca/K and Cl/K ratios implies that K-poor plagioclase clasts are the source.

We conclude that the young extrapolated radiogenic age of ca. 570 ka represents the age of frictional melting at this locality. Furthermore, the well-defined correlations between apparent age values, matrix abundance, and K content clearly indicate that they belong to the same genetic group of veins that formed under similar conditions and crustal depths. Adopting a 6–9 mm/yr exhumation rate for the last 1 m.y. (Little et al., 2005), the interpreted age of frictional melting can be used to constrain the depth of paleoseismic faulting to ~3.5–5 km.

Interestingly, all total gas ages measured were to some degree contaminated with inherited Ar, despite efforts to preselect matrix-rich portions of the veins for isotopic analysis. Even the total gas ages of samples that showed minimal influence from clast components with low Ca/K (<0.4) and Cl/K (0.04) ratios did not give exact ages of friction melting. Only a hypothetical Ca/K value of zero, which presumably would represent a plagioclase-free vein, yielded a total gas age intercept value close to that of friction melt generation (Fig. 3D). The occurrence of four pseudo-plateau "apparent age" spectra characterized by constant degassing behavior over 35%–60% of the release spectra also appears to have little chronological meaning in these samples.

Our study shows that age and formation depth of pseudotachylytes can be reliably constrained by the relationships between isotopic age values, percent melted matrix, and K content. Varying ages do not negate the use of the Ar method but show a progression toward complete melting of host rock that can be extrapolated and quantified. The results show that accurate and meaningful age values for friction melt events can be obtained by laser-ablation $^{40}Ar/^{39}Ar$ step-heating analysis of genetically related veins systems or portions of the same vein that vary in matrix-clast percentage. Improvements in the dating of these rocks would benefit considerably by preselection of samples based on textural and chemical characterization prior to time-consuming isotopic analyses.

ACKNOWLEDGMENTS

The $^{40}Ar/^{39}Ar$ isotopic analyses, electron microscopy, and inductively coupled plasma–optical emission spectroscopy (ICP-OES) analyses were carried out at the University of Michigan. We thank Chris Hall and Ted Huston for technical support and Joel Blum for access to his inductively coupled plasma facility. Research was supported by grants from the U.S. National Earthquake Hazards Reduction Program (USGS-04HQGR0066) and the U.S. National Science Foundation (EAR-0230055 and 0345985). Rick Simpson and Simon Cox are thanked for helpful discussions and logistical support, and Laura Webb, Sara Sherlock, and John Spray provided constructive reviews.

REFERENCES CITED

Adams, C.J., 1981, Uplift rates and thermal structure in the Alpine fault zone and Alpine schists, Southern Alps, New Zealand: Geological Society of London Special Publication 9, p. 211–222.

Batt, G.E., Braun, J., Kohn, B.P., and McDougall, I., 2000, Thermochronological analysis of the dynamics of the Southern Alps, New Zealand: Geological Society of America Bulletin, v. 112, p. 250–266, doi: 10.1130/0016–7606(2000)112<0250:TAOTDO>2.3.CO;2.

Cooper, A.F., and Norris, R.J., 1994, Anatomy, structural evolution, and slip rate of a plate-boundary thrust: The Alpine fault at Gaunt Creek, Westland, New Zealand: Geological Society of America Bulletin, v. 106, p. 627–633, doi: 10.1130/0016–7606(1994)106<0627:ASEASR>2.3.CO;2.

Di Toro, G., Hirose, T., Nielsen, S., Pennacchioni, G., and Shimamoto, T., 2006, Natural and experimental evidence of melt lubrication of faults during earthquakes: Science, v. 311, p. 647–649, doi: 10.1126/science.1121012.

Di Vincenzo, G., Rocchi, S., Rossetti, F., and Storti, F., 2004, ^{40}Ar-^{39}Ar dating of pseudotachylytes: The effect of clast-hosted extraneous argon in Cenozoic fault-generated friction melts from the West Antarctic rift system: Earth and Planetary Science Letters, v. 223, p. 349–364, doi: 10.1016/j.epsl.2004.04.042.

Grapes, R.H., 1995, Uplift and exhumation of Alpine schist, Southern Alps, New Zealand: Thermobarometric constraints: New Zealand Journal of Geology and Geophysics, v. 38, p. 525–533.

Kohut, M., and Sherlock, S., 2003, Laser microprobe ^{40}Ar-^{39}Ar analysis of pseudotachylyte and host-rocks from the Tatra Mountains, Slovakia: Evidence for late Paleogene seismic/tectonic activity: Terra Nova, v. 15, no. 6, p. 417–424, doi: 10.1046/j.1365–3121.2003.00514.x.

Little, T.A., Cox, S., Vry, J.K., and Batt, G., 2005, Variations in exhumation level and uplift along the oblique-slip Alpine fault, central Southern Alps, New Zealand: Geological Society of America Bulletin, v. 117, p. 707–723, doi: 10.1130/B25500.1.

Lo Bello, Ph., Fraud, G., Hall, C.M., York, D., Lavina, P., and Bernat, M., 1987, $^{40}Ar/^{39}Ar$ step-heating and laser fusion dating of a Quaternary volcano from Neschers, Massif Central, France: The defeat of xenocrystic contamination: Chemical Geology, v. 66, p. 61–71.

Magloughlin, J.F., and Spray, J.G., 1992, Frictional melting processes and products in geological materials: Introduction and discussion: Tectonophysics, v. 204, p. 197–204, doi: 10.1016/0040–1951(92)90307-R.

Magloughlin, J.F., Hall, C.M., and van der Pluijm, B.A., 2001, ^{40}Ar-^{39}Ar geochronometry of pseudotachylytes by vacuum encapsulation: North Cascade Mountains, Washington, USA: Geology, v. 29, p. 51–54, doi: 10.1130/0091–7613(2001)029<0051:AAGOPB>2.0.CO;2.

Masch, L., Wenk, H.R., and Preuss, E., 1985, Electron microscopy study of hyalomylonite: Tectonophysics, v. 115, p. 131–160, doi: 10.1016/0040–1951(85)90103–9.

Merrihue, C., and Turner, G., 1966, Potassium-argon dating by activation with fast neutrons: Journal of Geophysical Research, v. 71, p. 2852–2857.

Mueller, W., Kelly, S.P., and Villa, I.M., 2002, Dating fault-generated pseudotachylytes: Comparison of $^{40}Ar/^{39}Ar$ stepwise-heating, laser-ablation and Rb-Sr microsampling analyses: Contributions to Mineralogy and Petrology, v. 144, p. 57–77.

Norris, R.J., and Cooper, A.F., 2001, Late Quaternary slip rates and slip partitioning on the Alpine fault, New Zealand: Journal of Structural Geology, v. 23, p. 503–520.

Pickard, A.L., Adams, C.J., and Barley, M.E., 2000, Australian provenance for Upper Permian to Cretaceous rocks forming accretionary complexes on the New Zealand sector of the Gondwanaland margin: Australian Journal of Earth Sciences, v. 47, p. 987–1007.

Sherlock, S.C., and Hetzel, R., 2001, A laser probe $^{40}Ar/^{39}Ar$ study of pseudotachylyte from the Tambach fault zone, Kenya: Direct isotopic dating of brittle faults: Journal of Structural Geology, v. 23, p. 33–44, doi: 10.1016/S0191–8141(00)00082–1.

Sibson, R.H., 1975, Generation of pseudotachylyte by ancient seismic faulting: Geophysical Journal of the Royal Astronomical Society, v. 43, p. 775–794.

Warr, L.N., and van der Pluijm, B.A., 2005, Crystal fractionation in friction melts of seismic faults (Alpine fault, New Zealand): Tectonophysics, v. 402, p. 111–124, doi: 10.1016/j.tecto.2004.12.034.

Warr, L.N., van der Pluijm, B.A., Peacor, D.R., and Hall, C.M., 2003, Frictional melt pulses during a ~1.1 Ma earthquake along the Alpine fault, New Zealand: Earth and Planetary Science Letters, v. 209, p. 39–52, doi: 10.1016/S0012–821X(03)00070–0.

Manuscript received 15 November 2006
Revised manuscript received 5 February 2007
Manuscript accepted 7 February 2007

Printed in USA